ELSEVIER

Journal of Power Sources 109 (2002) 136–141

JOURNAL OF POWER SOURCES

www.elsevier.com/locate/jpowsour

Improvement in electrochemical properties of nano-tin-polyaniline lithium-ion composite anodes by control of electrode microstructure

Xiang-Wu Zhang[a,*], Chunsheng Wang[a], A. John Appleby[a], Frank E. Little[b]

[a]*Center for Electrochemical Systems and Hydrogen Research, Texas Engineering Experiment Station, Texas A&M University, College Station, TX 77843-3402, USA*

[b]*Center for Space Power, Texas Engineering Experiment Station, Texas A&M University, College Station, TX 77843-3118, USA*

Received 17 December 2001; accepted 17 January 2002

Abstract

Four different types of nano-tin-polyaniline (nano-Sn-PAni) lithium-ion composite anode microstructures have been examined to investigate the relationship between this parameter and anode characteristics. Scanning electron microscopy (SEM) and electrochemical impedance spectroscopy (EIS) show that the electrochemical properties of nano-tin composite electrodes can be significantly affected by microstructure variation. To simultaneously obtain high capacity and long cycle life, the active materials should be encased in a polymer matrix to accommodate volume changes during cycling, and porosity is required to offer low interfacial lithium insertion/extraction impedance. The polymer matrix should have a high binding strength to prevent the anode cracking.

Keywords: Nano-tin; Polyaniline; Composite electrode; Charge–discharge; Cycle life

1. Introduction

Li-metal storage anodes for secondary Li-ion cells have been extensively studied since Dey demonstrated the feasibility of electrochemical insertion of Li in liquid organic electrolytes in early 1970s [1]. Lithium storage in host metals overcomes the problem of solvent co-intercalation with carbonaceous anodes, where it often results in large irreversible capacities [2,3]. Another advantage of Li-in-metal over carbon anodes is their much higher Li packing density and hence higher electrochemical capacity [4,5]. However, the higher Li packing density results in a large volume change on insertion, which causes anode cracking or pulverization [6]. Therefore, the control of volume changes during Li insertion/extraction is a key issue in the development of Li-metal anodes.

Various attempts have been applied to minimize the mechanical stress due to the large volume change by stabilizing microscopic morphology to improve electrochemical properties, especially cycle life. The methods most widely studied include limiting the degree of charge [7,8], the use of small particle size active material [9,10], the use of intermetallic and/or composite host material instead of pure metal [11–13], and the use of anodes bonded by conductive polymers [13,14]. Of these, composite anodes consisting of small particle-size Li-metal mechanically bonded by flexible conductive polymers should be attractive anode candidates. The polymer may not only include intrinsically conducting and/or doped materials, but also inert polymer composites filled with conducting particles, e.g. nickel-filled polyethylene (PE) [15]. In Li-metal conductive polymer composite anodes, the polymer matrix not only offers conductive pathways between the active storage material, current collector and electrolyte, but also accommodates the active material volume change via the polymer viscoelasticity. Finally, the use of active materials of small particle size may minimize any large absolute volume changes. This will also result in a longer cycle life.

The influence of the preparative procedure on the electrochemical performance of composite anodes has been reported, and it has been shown that their microstructure plays an important role in defining electrode characteristics [16–19]. However, these studies do not define a direction for optimization. In this paper, four typical types of nano-tin-polyaniline (nano-Sn-PAni) composite electrodes with various microstructures were prepared and their electrochemical performance investigated. The intrinsic electronic (semi)conductor PAni was used as the polymer matrix because of its ease of fabrication, high conductivity when

* Corresponding author. Tel.: +1-979-845-8281; fax: +1-979-845-9287.
E-mail address: xwzhang@tamu.edu (X.-W. Zhang).

0378-7753/02/$ – see front matter
PII: S0378-7753(02)00091-5

doped, excellent stability [20,21], and the ease by which it may be used to prepare composite anodes of varying microstructure. Unlike other common polymer binders, it requires no conducting additives and so is able to give high interparticle binding strength to accommodate the large absolute volume change in the active materials.

2. Experimental

2.1. Electrode preparation

Nano-Sn power (Argonide Corporation, Sanford, FL) of 98 nm mean particle diameter was used as the active material. The polymer matrices were emeraldine base PAni (EB, Aldrich Chemical) with molecular weights of 10,000 (PAni-1), 20,000 (PAni-2) and 65,000 (PAni-3) doped (see following sections) with lithium hexafluorophosphate ($LiPF_6$, Aldrich Chemical) to give the corresponding highly-conducting emeraldine salts (ES) with one Li^+ per two aniline units. Their conductivities were 8.7, 2.9 and 5.4 S cm^{-1}, respectively.

Four types of composite anodes were prepared using procedures given in Fig. 1. For type I anodes, the $LiPF_6$ was added into a 1-methyl-2-pyrrolidone (NMP) solution of PAni, which was stirred for 30 min, cast onto glass, and dried at 75 °C for 17 h. The film was then finely ground, mixed with nano-Sn powder, and pressed at 100 MPa onto a copper gauze to give finished type I anodes. In type II, the nano-Sn, PAni and $LiPF_6$ were added to NMP simultaneously, then stirred for 30 min, and cast directly on the copper gauze to form the anodes, which were dried at 75 °C for 17 h. In type III, Sn-doped–PAni composite films were cast as in type I from the mixture prepared as in type II. These were finely ground, and pressed at 100 MPa onto copper gauges at room temperature. Type IV anodes were prepared as in type III, except that the temperature used during pressing was 210 °C for PAni-2 and PAni-3, and 100 °C for the lower-melting PAni-1.

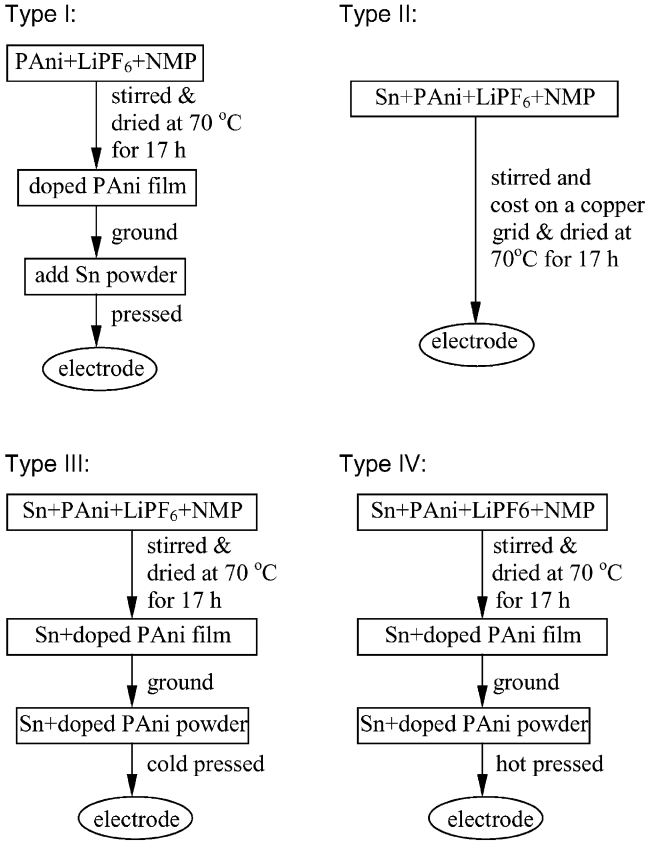

Fig. 1. Preparative routes for four types of composite anodes.

The active materials content in all anodes was fixed at 80 wt.%. Microstructure was determined by JSM-6400 scanning electron microscopy (SEM).

2.2. Electrochemical measurement

Charge–discharge behavior was examined in a three-electrode PTFE cell containing excess 1.0 M $LiPF_6$ in 4:1:3:2 by volume ethylene carbonate (EC)–propylene carbonate (PC)–dimethyl carbonate (DMC)–ethyl methyl carbonate (EMC) mixture (Em Industries, Inc.) as electrolyte. Two lithium foils were used as counter and reference electrodes. All potentials given are versus Li/Li^+ in this electrolyte. Cells were assembled in an argon-filled glove box. Charge (lithium insertion) and discharge (lithium extraction) were conducted on an Arbin (College Station, TX) automatic battery cycler at current densities of 5.0 mA g^{-1} with cut-off potentials of 0.0 and 1.5 V.

Electrochemical impedance spectroscopy (EIS) was performed using a Solarton FRA 1250 frequency response analyzer and a Solarton model 1286 electrochemical interface. Before each measurement, the electrodes were first charged (galvanostatically at 5 mA g^{-1}) to 0.0 V, then left on open-circuit for 5.0 h to allow their potential to stabilize. EIS measurements were then carried out using a 5.0 mV ac voltage signal in the 65 kHz–10 mHz frequency range in automatic sweep mode from high to low frequency.

3. Results and discussion

3.1. Influence of molecular weight of PAni matrix

Microstructure plays an important role in the electrochemical performance of secondary electrodes. At a given anode composition, microstructure should be optimized to simultaneously produce electrodes with high capacity and long cycle life. Fig. 2 shows the potential profiles of the first three cycles for the four classes of anodes. During charge, the potentials for all anodes fall rapidly down to 0.3–0.4 V, then slowly decreased to 0.0 V. During discharge, potentials increased rapidly to about 0.4 V, then plateaus appear. Other work has indicated that cathodic Li^+ extraction from PAni

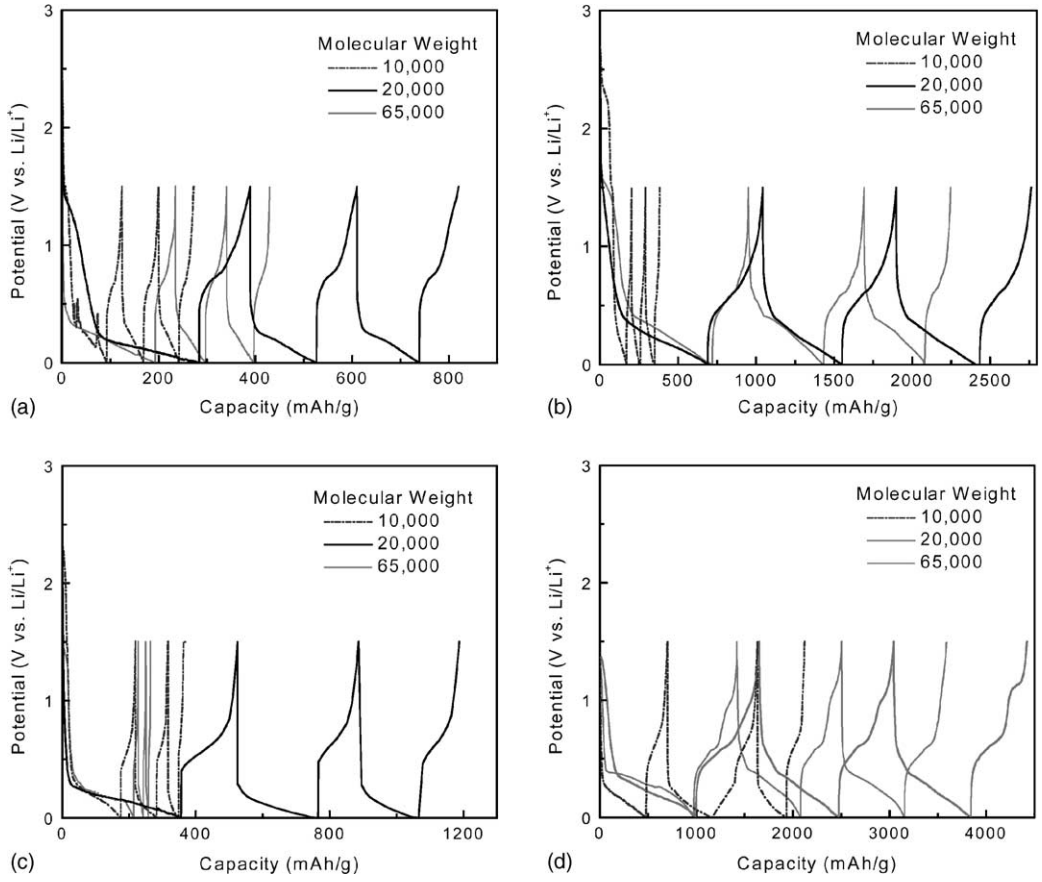

Fig. 2. Charge–discharge curves for nano-Sn-PAni composite anodes with differing microstructures: (a) type I; (b) type II; (c) type III; and (d) type IV. The capacities are given with respect to the mass of active materials in the anodes.

occurs at over 2.5 V [22], so the capacities shown in Fig. 2 are those for anodic Li insertion/extraction to/from nano-Sn particles in the potential range 0.0–1.5 V. However, capacities were strongly dependent on PAni matrix molecular weight. Fig. 2 shows that only PAni-2 bonded anodes have high charge/discharge capacities. The melting point for low molecular weight (10,000 Da) PAni-1 is only 160 °C, whereas those for PAni-2 and PAni-3 are greater than 350 °C. The short chain of the PAni-1 macromolecule results in bonding incapable of counteracting the mechanical stress resulting from the nano-Sn volume changes, and consequent loss of particle–particle contact results in very low capacities. The very long chains of PAni-3 are not completely soluble in NMP, and anodes containing it are too brittle to accommodate volume changes. Only, the medium-range molecular weight PAni-2 has the correct mechanical properties to strongly bind the nano-Sn particles and counteract their expansion/contraction.

3.2. Influence of composite electrode microstructure

In general, composite anodes containing PAni-2 show relatively high capacity, but it is clear that capacities, i.e. Li insertion/extraction rates, are controlled by kinetics across the active particle/electrolyte interface. Long-term cycling performance is largely determined by PAni matrix binding strength, which counteracts volume changes. Because the anode and electrolyte compositions studied were fixed, both of the above factors are only associated with the electrode microstructures. Fig. 2 shows that charge/discharge capacities vary greatly with anode type. Using PAni-2 anodes as an example, type I has the lowest initial charge capacity (283 mAh g^{-1}), while that of type IV is about 3.5 times larger at 997 mAh g^{-1}. Those of types III and II are 347 and 688 mAh g^{-1}, respectively. The reversible discharge capacities show a similar trend, with 105, 168, 348 and 655 mAh g^{-1} for types I, III, II and IV, respectively.

The anode type, i.e. its microstructure (see following sections), not only affects charge/discharge capacity during the first few cycles, but also largely determines its long-term cycling performance, which in turn determines the suitability of Li-alloy anodes for secondary Li-ion cells. Cycling performances as capacities and efficiencies for different anode types are shown in Fig. 3a and b, respectively. Types I and III capacities were very low and their cycle lives were too short for practical application. Type II anodes had better cycling performance, i.e. capacity loss before the 70th cycle was small, but their charge/discharge capacities were still unsatisfactory. In contrast, type IV gave charge discharge capacities of 450 and 400 mAh g^{-1}, respectively, until

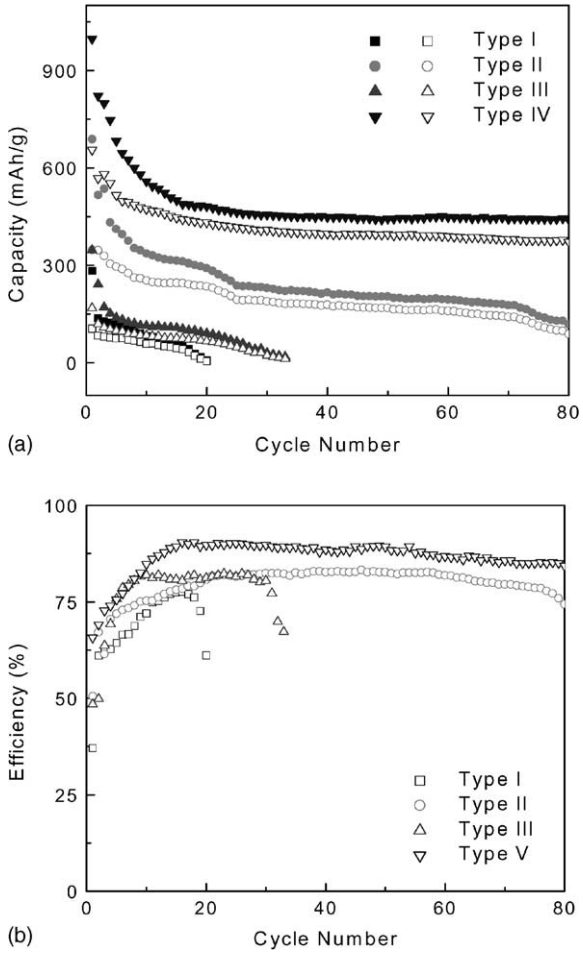

Fig. 3. Cycling behaviors of nano-Sn-PAni composite anodes with differing microstructures: (a) charge (solid symbols) and discharge (open symbols) capacities with respect to the mass of active material. (b) Corresponding efficiencies.

the 80th cycle. Fig. 3a shows that irreversible capacity is observed for all anodes. Charge/discharge efficiencies increase during the first 10 cycles to an equilibrium value, after which they abruptly decrease on a given cycle on mechanical breakdown of the anode (Fig. 3b). The progression of capacity and efficiency show that the cycle lifetimes (in increasing order) are the same as for capacities, i.e. type I < type III < type II < type IV.

3.3. SEM and EIS measurements

To clarify the effect of anode microstructure on charge/discharge capacities and cycling performance, the morphologies of uncycled composite anodes were imaged by SEM (Fig. 4). Fig. 4a clearly shows that the nano-Sn particles in type I anodes exposed at the electrode surface are not coated by the PAni matrix. The surface is also very porous. The preparation of type I anodes involved simple blending of doped PAni and nano-Sn powders, so the active particles not coated by PAni. The exposed Sn particles have only a small contact area with the PAni matrix, which cannot oppose the large mechanical stresses due to volume changes in the active particles during cycling. This results in pulverization and/or cracking of both active materials and anodes, giving low capacities and poor cycle life. Anode microstructure also influences the electrode–electrolyte interfacial process, as EIS measurement shows. Typical impedance spectra (Fig. 5) all show one depressed semicircle for the interfacial impedance, which is usually taken to be for interfacial Li charge transfer associated with the formation of the passive surface electrode interface (SEI) film. Fig. 5 shows that interfacial impedance of type I anodes is very low, indicating rapid Li insertion–extraction kinetics resulting from the high anode porosity, which allows electrolyte to penetrate the electrode interior. The lack of coating allows direct active particle to electrolyte contact, which further lowers impedance. However, pulverization and/or cracking of the active material and/or the anode limits type I capacity and cycle lifetime. This demonstrates that accommodation of the active material volume change and rapid Li insertion–extraction of lithium must be simultaneously presented in optimized anodes.

In type II electrodes, the Sn particles were first dispersed in the NMP solution of doped PAni, which was then directly dried to form the anodes. Here, no surface porosity is observed, and the Sn particles are totally coated by doped PAni (Fig. 4b). This dense strongly-bonded structure can accommodate the active material volume change, giving much longer cycle lifetimes. However, its very low porosity results in poor Li insertion/extraction kinetics, as is shown by the high interfacial impedance in Fig. 5. This results in a low charge/discharge capacity.

For the preparation of type III anodes, the type II anode materials were finely ground, then pressed to form electrodes at room temperature. Fig. 4c shows that the Sn particles in type III anodes are coated by doped PAni to form large composite particles which are bound together, with porosity in between. This permits electrolyte to penetrate the anode, diminishing the interfacial impedance (Fig. 5), enhancing interfacial mass transport and capacity. The electrodes were pressed at room temperature (at 0.69 K of the melting point), so the flow and sintering of polymer is slow under these conditions. Hence, little bonding by the macromolecular chains occurs between ground powder particles, so the overall binding strength of the anode is very low. As a result, the mechanical stress induced by active materials volume changes cannot be accommodated, and cracking occurs, so both capacities and cycling life are low.

Type IV electrodes were pressed from type II powders at high temperatures (at 0.86 K of the melting point for PAni-1, and 0.75 K for PAni-2 and PAni-3). Sintering under these conditions allows the macromolecular chains to bind the electrode strongly [23], giving denser anodes with smaller pores than type III (Fig. 4d). While not as strongly bound as type II, the PAni matrix can at least partially accommodate the mechanical stress, and the anode porosity also helps to

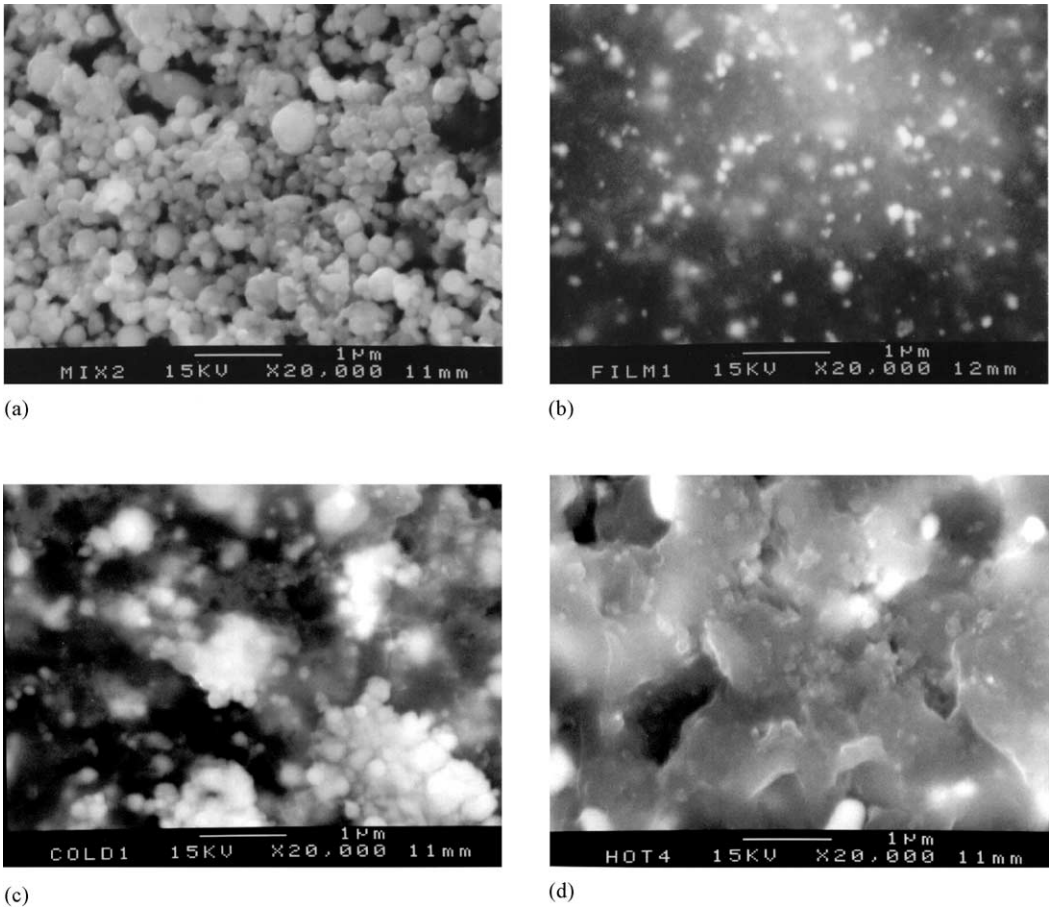

Fig. 4. SEM micrographs of nano-Sn-PAni composite anodes with differing microstructures: (a) type I; (b) type II; (c) type III; and (d) type IV.

provide space for the volume change. Thus, the cycle lifetime of type IV anodes is very good. The existence of porosity also gives a low interfacial resistance (Fig. 5), hence, a very high capacity (see Figs. 2 and 3).

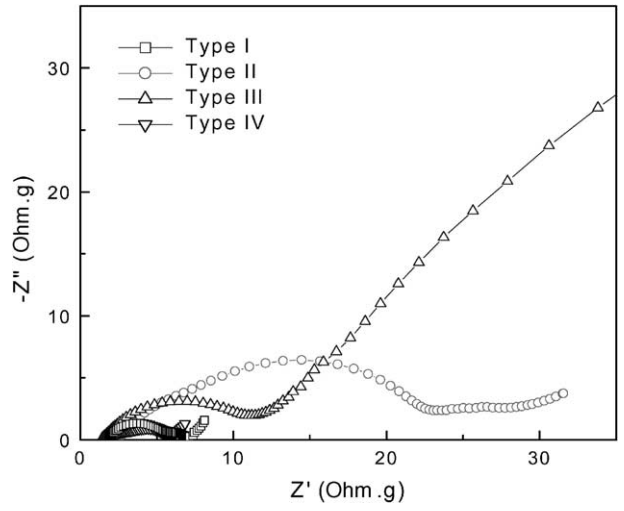

Fig. 5. Electrochemical impedance spectra of nano-Sn-PAni anodes with differing microstructures. Before measurements, the anodes were first charged at 5 mA g^{-1} to 0.0 V, then allowed to relax at open-circuit for 5.0 h.

Hence, to achieve both high capacities after long times and a long cycle life in composite anodes, stable porosity is required to accelerate mass transport through the active particle–electrode–electrolyte interfaces, and the binding strength of the polymer matrix onto the active material must be sufficient to accommodate the volume changes on cycling. The latter is the key mechanical issue for long cycle lifetimes. Thus, an optimum structure between the extremes of a solid anode and a porous structure is required. We should note that porosity in an anode of type IV will not be effective when a solid electrolyte is used. The latter will limit the capacity and charge rate of the type IV anode, which has both high capacity and long cycle lifetime in liquid electrolytes. The type II anode prepared by casting fits the solid electrolyte application, but its high interfacial impedance will limit its charge/discharge capacity.

4. Conclusions

The large volume change of a metal host during Li insertion–extraction represents a challenge for the application of Li-metal storage in secondary Li-ion cells. At the same time, means to accelerate interfacial Li insertion/extraction must be sought to achieve high capacity and rate

capability. This work shows the anode microstructure can be controlled to simultaneously perform both of the earlier, and thus, improve capacity and cycle performance. Four types of nano-Sn-PAni composite anodes containing polymers of differing molecular weights and with different microstructures were prepared to investigate the influence of these parameters on their electrochemical properties. The type I electrode, whose active storage material was exposed to the electrolyte, had the lowest capacities due to poor particle-to-particle contact and gave the shortest cycle life. The dense film type II anode without porosity showed much longer cycle life, but its capacity was unsatisfactory. The type III anode pressed from powdered composite at room temperature had both low capacity and a short cycle life because of its poor binding strength. The type IV prepared from sintered composite powders showed much higher capacities and longer cycling life than the other three types. This is explained by its multi-porosity structure and high binding strength. Low molecular weight polymer (10,000 Da) showed poor electrochemical properties due to its low binding strength, whereas high molecular weight (65,000 Da) material was not only incompletely soluble, but produced brittle electrodes which cracked and gave poor cycle life. The most satisfactory electrodes were made from material with a molecular weight of 20,000 Da.

Acknowledgements

We gratefully acknowledge NASA-Glenn Research Center (Grant no. NAG3-2617) for supporting this work.

References

[1] A.N. Dey, J. Electrochem. Soc. 118 (1971) 1547.
[2] M. Winter, P. Novak, A. Monnier, J. Electrochem. Soc. 145 (1998) 428.
[3] A.N. Dey, B.P. Sullivan, J. Electrochem. Soc. 117 (1970) 222.
[4] R. Nesper, Prog. Solid State Chem. 20 (1990) 1.
[5] J.O. Besenhard, J. Yang, M. Winter, J. Power Sources 68 (1997) 87.
[6] R.A. Huggins, Solid State Ionics 57 (1998) 113.
[7] J.R. Owen, W.C. Maskell, B.C.H. Steele, T.S. Nielsen, O.T. Sorensen, Solid State Ionics 13 (1984) 329.
[8] W.C. Maskell, J.R. Owen, J. Electrochem. Soc. 132 (1985) 1602.
[9] M. Winter, J.O. Besenhard, Electrochem. Acta 45 (1999) 31.
[10] J. Yang, M. Winter, J.O. Besenhard, Solid State Ionics 90 (1996) 281.
[11] Y. Idota, T. Kubota, A. Matsufuji, Y. Maekawa, T. Miyasaka, Science 276 (1997) 1395.
[12] O. Mao, R.A. Dunlap, J.R. Dahn, J. Electrochem. Soc. 146 (1990) 405.
[13] M. Maxfield, T.R. Jow, S. Gould, M.G. Sewchok, L.W. Shacklette, J. Electrochem. Soc. 135 (1988) 299.
[14] T.R. Jow, L.W. Shacklette, J. Electrochem. Soc. 136 (1989) 1.
[15] J. Yang, Y. Takeda, N. Imanishi, T. Ichikawa, O. Yamamoto, Solid State Ionics 135 (2000) 175.
[16] M. Wachtler, M.R. Wagner, M. Schmied, M. Winter, J.O. Besenhard, J. Electroanal. Chem. 510 (2001) 12.
[17] K.M. Kim, W.S. Jeon, I.J. Chung, S.H. Chang, J. Power Sources 83 (1999) 108.
[18] C.Y. Yang, C.H. Cheng, S.M. Ho, J.C. Chen, W.M. Hurng, J. Power Sources 68 (1997) 440.
[19] Y. Sato, T. Nakano, K. Kobayakawa, T. Kawai, A. Yokoyama, J. Power Sources 75 (1998) 271.
[20] J.Y. Shimano, A.G. MacDiarmid, Synth. Met. 123 (2001) 251.
[21] K.S. Ryu, B.W. Moon, J. Joo, S.H. Chang, Polymer 42 (2001) 9355.
[22] K.S. Ryn, K.M. Kim, S.G. Kang, G.J. Lee, S.H. Chang, Solid State Ionics 135 (2000) 229.
[23] X.-W. Zhang, L. Shen, X.S. Yi, Mater. Rev. 13 (46/47) (1999) 70.